Transp Porous Med (2013) 97:223–239
DOI 10.1007/s11242-012-0119-5

A Benchmark Solution for Infiltration and Adsorption of Polluted Water Into Unsaturated–Saturated Porous Media

Jozef Kačur · Jozef Minár

Received: 14 May 2012 / Accepted: 21 December 2012 / Published online: 10 January 2013

Abstract We discuss the numerical modeling of the infiltration of contaminated water into unsaturated porous media. A system with contaminant transport, dispersion, and adsorption is considered. The mathematical model for unsaturated flow is based on Richards nonlinear and degenerate equation. Nonlinear adsorption is represented by adsorption isotherms and kinetic rates. An accurate numerical method is constructed in 1D which can be a good candidate for the solution of inverse problems to determine model parameters in the adsorption part of the model. Our numerical solution is based on the method of lines (MOL method) where space discretization leads to the corresponding system of ODEs. We substantially use the numerical modeling of interfaces, separating fully saturated, partially saturated, and dry zones in the underground. Finally, in a series of numerical experiments and in comparisons with HYDRUS (Šimunek et al., The HYDRUS-1D software package for simulating the one-dimensional movement of water, heat, and multiple solutes in variably/saturated media, version 2.0, Rep. IGWMC-TPS-70, 202 pp., Int. Groundwater Model. Cent., Colo. Sch of Mines, Golden, Colo), we demonstrate the effectiveness of our method.

Keywords Contaminant Transport · Unsaturated flow · Nonlinear adsorption · Numerical modelling of contaminant transport

1 Introduction

The protection of clean water in aquifers represents an important part in many research teams' projects. Many scientists and engineers focus on this field. Numerous monographs and articles, appeared over the last decade, have significantly contributed to this field. The

J. Kačur (✉) · J. Minár
Faculty of Mathematics, Physics and Informatics, Comenius University, Mlynska dolina, 84248 Bratislava, Slovakia
e-mail: Kacur@fmph.uniba.sk

J. Minár
e-mail: jozef.minar@fmph.uniba.sk

contaminated surface water infiltrates into the unsaturated underground and there, the contaminant dissolved in the water obeys a complex of geophysical and geochemical processes. Many mathematical models describe them realistically (see Sun 1966) and there are many numerical methods for their realization (see e.g., Sun 1994; Šimunek and Nimo 2005; Bitterlich and Knabner 2002; Krutle and Knabner 2007; Krutle and Knabner 2005; Totsche et al. 1996; Bitterlich et al. 2004 etc.). We consider mathematical models describing advection, dispersion-diffusion, and adsorption of a contaminant. In fact, these mathematical models include a lot of data (hydrological and geochemical) strongly related to the specific site where the model is applied. These data have to be measured and some of them have to be determined by solving the inverse problems (via black box) when additional measurements of some characteristics are available. Some of these model data (e.g., soil parameters in capillary pressure and hydraulic permeability dependence in terms of saturation, adsorption isotherms) can be obtained in laboratory conditions with 1D samples (using tubes of the corresponding underground)—see, e.g., Sun (1994), Šimunek and Nimo (2005), Totsche et al. (1996), Bitterlich et al. (2004), Kacur et al. (2005), and citations there. Then they can be used in complex 3D models. The solution of the inverse problem requires a very accurate and effective numerical solution of the direct problem. The main goal of our contribution is to propose such a numerical method in 1D. In our contribution we focus on the numerical modeling of contaminant transport with adsorption in unsaturated-saturated porous media. The corresponding mathematical model is strongly nonlinear, linking advection, diffusion-dispersion, and adsorption together. Especially, when the contaminated water infiltrates into the originally dry porous media, there appear saturated, partially saturated, and (remaining) dry zones, separated by moving interfaces. These interfaces are implicitly included in the solution, although they are not known originally. Moreover, the contaminant dissolved in the water can also generate zones where it is present or absent, due to (generally) nonlinear adsorption (Kacur et al. 2010). It is well-known that the front of saturation in the neighborhood of a dry zone is very sharp. Hence, it is very difficult to approximate its derivatives (see Constales and Kacur 2004) since they can be unbounded at the interface. Application of moving grid points in numerical approximation is desirable. There are some strategies for the construction of moving grid points. One was applied in, e.g., Kacur et al. (2010), where the nonlinear adsorption and diffusion problem in a fully saturated porous media was considered. Implementation of this discretization strategy would decrease the effectiveness of our method significantly. Our construction of moving grids is strongly linked to the moving interfaces. The system for water infiltration into the dry region is governed by the strongly nonlinear and degenerate Richards equation ("porous media type equation") which gives rise to two interfaces. Once we know the evolution of the wetness front, we solve our mathematical model only in the moving domain bounded by this front. Moreover, we can easily construct moving grids linked only with this moving front. We have developed a mathematical model for the time evolution of these (full saturation and wetness) interfaces. They are substantially used in the construction of moving grids which "follow" these interfaces; thus we obtain accurate numerical approximations (of gradients of unknowns) for the considered time interval. We demonstrate the accuracy of our computations in numerical experiments by controlling the water and contaminant mass balances. Also, comparisons of our results with those obtained by the well-tested and widely used software HYDRUS are very important. Although this numerical method is completely different from ours, the results of both methods are in good agreement. This gives additional support for our method. We discuss the comparison of both methods in Sect. 4.1. Some numerical experiments with our method are presented in Sect. 4.2.

2 Mathematical Model

The mathematical model for the convection-diffusion-adsorption of the contaminant is based on the Fick's law and the mass balance argument. The flow in unsaturated porous media is modeled by the hydraulic conductivity K, where $K(h) = K_s \cdot k(h)$ and $k(h)$ is a function describing the dependency of the conductivity on the pressure head h, or on the corresponding effective saturation (see van Genuchten 1980). Here, K_s is the hydraulic conductivity in fully saturated porous media,

$$K_s = \kappa_0 \frac{\rho g}{\mu}, \tag{1}$$

where ρ and μ are the density and the dynamical viscosity of the water, respectively. The coefficient κ_0 depends only on the structure of the porous medium and g is the gravitational acceleration. Richards equation in the unsaturated zone can be written in terms of saturation θ and reads as

$$\partial_t \theta = \operatorname{div}(K(h)\nabla(h+z)), \tag{2}$$

where $K(h)$ is expressed in terms of effective saturation u (rescaled θ)

$$u = \frac{\theta - \theta_r}{\theta_0},\ \theta_0 = \theta_s - \theta_r \tag{3}$$

and reads as

$$K(h) = K_s k(u), \quad k(u) = u^{\frac{1}{2}}(1 - (1 - u^{\frac{1}{m}})^m)^2. \tag{4}$$

Here, θ_s and θ_r are fully saturated and residual water contents, respectively. We consider the capillary pressure model in the following form:

$$u = \frac{1}{(1 + (\alpha h)^n)^m}, \tag{5}$$

where $n > 1, m = 1 - \frac{1}{n}$ and $\alpha < 0$ are the soil parameters in the van Genuchten–Mualem (empirical) model.

There are also other models (Brooks and Corey, Brutsaert, Vauclin), but we will use the van Genuchten–Mualem model, because the fundamental relations (hydraulic conductivity versus saturation and saturation versus head) reflect the appearance of interfaces separating saturated, partially saturated, and dry zones. The contaminant transport is the superposition of advective and diffusive-dispersion parts—see Sun (1966). Darcy's discharge is given by $\mathbf{v} = -K(u)\nabla(h+z)$ and the corresponding contaminant flux is given by

$$\mathbf{J}_{\text{adv}} = \mathbf{v}w, \tag{6}$$

where w is the concentration of the contaminant dissolved in the water. We assume isotropy and homogeneity of the porous medium. Due to the diffusion-dispersion, the contaminant flux is given by

$$\mathbf{J}_{\text{dis}} = -\theta \mathbf{D} \cdot \nabla w. \tag{7}$$

Here, $\mathbf{D}$ is a positive definite symmetric matrix. The components of $\mathbf{D}$ can be expressed as

$$D_{ij} = (D_0 + \alpha_T |\mathbf{v}|)\delta_{ij} + \frac{v_i v_j}{|\mathbf{v}|}(\alpha_L - \alpha_T), \tag{8}$$

where α_L, α_T are longitudinal and transversal dispersivities, respectively, δ_{ij} is the Kronecker delta, and D_0 is the molecular diffusion coefficient.

Using the mass balance equation for the total flux $\mathbf{J} = \mathbf{J}_{\text{adv}} + \mathbf{J}_{\text{dis}}$ we get the equation for the transport of the contaminant with diffusion,

$$\frac{\partial(\theta w)}{\partial t} = -\nabla \cdot \mathbf{J}, \tag{9}$$

which leads to the well-known *convection-diffusion* equation

$$\partial_t(\theta w) + \operatorname{div}(\mathbf{v}w - \theta \mathbf{D}\nabla w) = -\rho \partial_t S. \tag{10}$$

The adsorption of the contaminant is governed by the equation (see, e.g., Knabner and van Duijn 1995; Constales et al. 2003)

$$\partial_t S = \kappa(\Psi(w) - S), \tag{11}$$

where S represents the adsorbed contaminant by a unit mass of porous media, κ is the adsorption rate coefficient, and Ψ represents an adsorption isotherm.

The mathematical model (11) is a very simple one where the most common isotherms can be considered (see, e.g., Totsche et al. 1996; Sun 1994; Knabner and van Duijn 1995; Constales et al. 2003):

$$\Psi(s) = as \text{(linear)};\ \Psi(s) = as^b \text{(Freundlich)};\ \Psi(s) = \frac{as}{1+bs} \text{(Langmuir)};$$

$$\Psi(s) = \frac{as^r}{1+bs^r} \text{(Mixed Freundlich-Langmuir)}.$$

In (11), the reversible adsorption mode is considered where the contaminant can be both fixed to the solid and dissolved back from the solid into the water. It is also possible to consider the irreversible model, where the contaminant cannot be dissolved back into the water. Then, the following modification of (11) can be used:

$$\partial_t S = \kappa \max(0, \Psi(w) - S). \tag{12}$$

Another extension can be considered, when some compounds of the solid matrix adsorb the contaminant in an equilibrium mode which corresponds to $\kappa \to \infty$. In that case we have $S = S_e = \Psi_e(s)$, where $\Psi_e(s)$ is the adsorption isotherm in the equilibrium mode and it can have one of the above-mentioned forms. In that case the R.H.S. term $\rho \partial_t S_e = \rho \partial_t \Psi_e(w)$ can be added to the term $\partial_t(\theta w)$ on the L.H.S. of (10). In general, the contaminant can be adsorbed both in the equilibrium and non-equilibrium modes. In that case (due to superposition) we obtain (11), where we replace $\partial_t(\theta w)$ by $\partial_t(\theta w + \rho \Psi_e(w))$. Then $\Psi(s)$ in (11) represents the adsorption isotherm in the non-equilibrium mode with the corresponding S—see Kacur et al. (2005), Knabner and van Duijn (1995), Kacur et al. (2010), Constales et al. (2003).

The presented model is completed by initial and boundary conditions. In our numerical experiments we approximate the system in the form (2), (10), (11).

The unsaturated-saturated flow in the sample is drawn in Fig. 1.

Remark 1 Our mathematical model can be extended to the case when K_s and θ_s are dependent on the amount of the adsorbed contaminant S. Then our system is strongly coupled and the flow part cannot be separated.

Remark 2 We note that our method together with the existing code could be extended to the case when more contaminants are dissolved in the water and obey chemical reactions. Consequently, our system would increase and it would be coupled with a system of algebraic equations. This can be solved by DAE solvers for stiff problems.

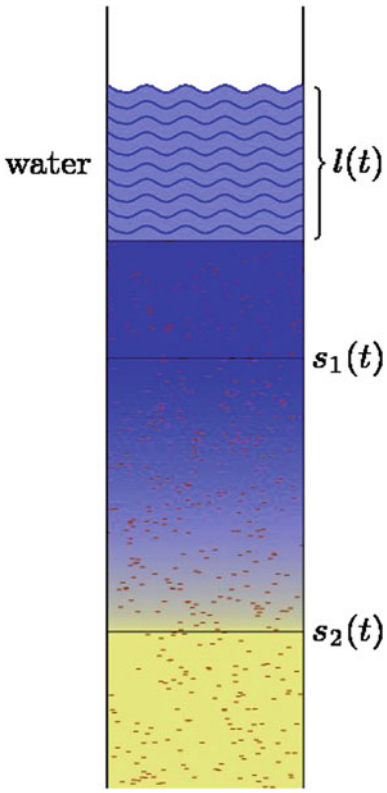

Fig. 1 Sketch of unsaturated/saturated flow in a sample

2.1 Stages in Our 1D Model and Corresponding Boundary Conditions

In our 1D model we assume that the domain is a sample (in the form of a tube). On its top there is an $\ell(t)$ column of contaminated water infiltrated (due to the gravitation and capillary forces) into the originally dry sample. On its bottom there is a tube where outgoing water flows out. We will denote by $\ell_2(t)$ the height of the outgoing water in the bottom tube (which has equal sectional area as the top column) and by S_{out} the total amount of the contaminant in this outgoing water. The whole process we are modeling, generally, undergoes different stages with different boundary conditions. Roughly speaking, these stages can be:

1. The water infiltrates into the sample and does not flow out.
2. The water does not infiltrate (the top column is empty) and does not flow out.
3. The water infiltrates into the sample and flows out from the sample at the same time, while the whole sample is not fully saturated.
4. The water infiltrates into the sample and flows out from the sample at the same time, while the whole sample is fully saturated.
5. The water does not infiltrate into the sample and the water flows out from the sample.

We briefly describe these stages in the next subsections, referring to each stage under the number it was noted here. Note that not all of these stages happen in one experiment (e.g., the experiment will start at Stage 1, continue with Stage 2, and end at Stage 5). Let us rewrite our governing ODEs in 1D:

$$\partial_t \theta = \partial_x (K(u)(\partial_x h - 1)) \tag{13}$$

$$\partial_t(\theta w) + \partial_x(qw - (D_0\theta + \alpha_L q)\partial_x w) + \rho \partial_t S = 0 \tag{14}$$

$$\partial_t S = \kappa(\Psi(w) - S), \tag{15}$$

where $q(x,t) = -K(u)(\partial_x h - 1)$, $K(u) = K_s u^{\frac{1}{2}}(1-(1-u^{\frac{1}{m}})^m)^2$, $u = \frac{\theta-\theta_r}{\theta_0}$,$\theta_0 = \theta_s - \theta_r$, and $\Psi(s) = as^b$.

2.1.1 Stage 1

In this stage there are two interfaces s_1 and s_2 in the sample. The interval $(0, s_1(t))$ represents the fully saturated zone of the sample, $(s_1(t), s_2(t))$ represents the partially saturated zone of the sample, and $(s_2(t), d)$ represents the dry zone, where d is the length of the sample. The flow model in the fully saturated zone is governed by Darcy's law ($u = 1$) in $(0, s_1(t))$ and the pressure head is positive and linear, satisfying $h(s_1(t), t) = 0$ and $h(0, t) = \ell(t)$. Since the water flux is constant along the whole domain $(0, s_1(t))$ we obtain

$$\partial_t \ell(t) = K_s \left(1 + \frac{\ell(t)}{s_1(t)}\right) \equiv -q(0,t). \tag{16}$$

To determine s_2 we follow the ideas in Constales and Kacur (2004) and Constales et al. (2003). The time evolution of the wetness front is strongly linked with local properties of the saturation profile at the wetness front and it is expressed in the form of an ODE:

$$\partial_t s_2(t) = -\frac{K_s m^2}{\alpha\theta_0(n-1)p}\partial_x u(1,t)^p, \quad p = \frac{1}{m} + \frac{1}{2}. \tag{17}$$

The mathematical model for the interface s_1 is based on the mass balance equation which can be simplified to the form

$$s_1(t) = -\frac{\ell(t)}{\partial_x^+ h(s_1(t), t)}. \tag{18}$$

Boundary conditions for the effective saturation in these interfaces are given by $u(s_1(t), t)$=1 and $u(s_2(t), t) = 0$. The condition for the concentration at $x = 0$ is derived from the mass balance of the contaminant and can be written as

$$q_w(0,t) = qw - (D_0\theta + \alpha_L q)\partial_x w|_{(x,t)=(0,t)} = -w_\ell(t)\partial_t \ell, \tag{19}$$

where $w_\ell(t)$ is the concentration of the infiltrating water at time t. Other boundary conditions are:

$$\partial_x^- w(s_1(t), t) = \partial_x^+ w(s_1(t), t), \tag{20}$$

$$\partial_x w(s_2(t), t) = 0. \tag{21}$$

2.1.2 Stage 2

In this stage there is only one interface s_2 separating the partially saturated zone and the dry zone. Conditions (17) and (21) are the same as in Stage 1, and we use new boundary conditions

$$\partial_x h(0,t) = 1, \tag{22}$$

$$q_w(0,t) = qw - (D_0\theta + \alpha_L q)\partial_x w|_{(x,t)=(0,t)} = 0. \tag{23}$$

2.1.3 Stage 3

In this stage there is only one interface s_1 separating the fully saturated zone and the partially saturated zone. Conditions (16), (18), (19), and (20) are the same as in Stage 1, while in the boundary condition (21) the interface $s_2(t)$ is replaced by the length of the sample d:

$$\partial_x w(d,t) = 0. \tag{24}$$

Additionally, we use

$$\partial_x \theta(d,t) = 0, \tag{25}$$
$$\partial_t \ell_2(t) = q(d,t) = K(h(d,t)), \tag{26}$$
$$\partial_t S_{out}(t) = q(d,t)w(d,t) = K(h(d,t))w(d,t). \tag{27}$$

2.1.4 Stage 4

In this stage there are no interfaces and the whole sample is fully saturated. We do not need to compute the saturation, we just compute the concentration and the adsorption. The condition (19) is the same as in Stage 1 and conditions (24), (27) are the same as in Stage 3. In the boundary condition (16) the interface $s_1(t)$ is substituted by the length of the sample d:

$$\partial_t \ell(t) = -K_s \left(1 + \frac{\ell(t)}{d}\right) \equiv -q(0,t). \tag{28}$$

We consider a new condition:

$$\partial_t \ell_2(t) = K_s \left(1 + \frac{\ell(t)}{d}\right) \equiv q(0,t). \tag{29}$$

Note that conditions (28) and (29) are linear and, therefore, we can solve them analytically:

$$\ell(t) = (\ell(t_1) + d)e^{\frac{K_s}{d}(t_1 - t)} - d \tag{30}$$
$$\ell_2(t) = \ell(t_1) + \ell_2(t_1) + d - (\ell(t_1) + d)e^{\frac{K_s}{d}(t_1 - t)} \tag{31}$$

2.1.5 Stage 5

In this stage there are no interfaces and the whole sample is partially saturated. Conditions (22) and (23) are the same as in Stage 2 and conditions (24), (25), (26), and (27) are the same as in Stage 3.

3 Numerical Method

3.1 Approximation of the Flow

Since the flow of the water is not affected by the contaminant transport in the chosen model, we first focus on the flow. In the partially saturated zone $(s_1(t), s_2(t))$ (we define $s_1(t) \equiv 0$ in the stage without inflow and $s_2(t) \equiv d$ in the stage with outflow) we transform the governing Richards equation to the fixed domain $y \in (0, 1)$ using the transformation

$$y = \frac{x - s_1(t)}{ss(t)}, \quad ss(t) = s_2(t) - s_1(t). \tag{32}$$

Moreover, we rewrite it in terms of saturation u since $0 < u < 1$

$$\partial_t u = \frac{K_s}{\theta_0 ss(t)} \partial_y \left(\frac{WD(u)}{ss(t)} \partial_y u - k(u) + \frac{1}{ss} (\partial_t s_1 (1-y) + \partial_t s_2 y \right) \partial_y u \tag{33}$$

where—see (5)

$$WD(u) := k(u) \frac{\partial h}{\partial u} \tag{34}$$
$$u = 1 \text{ for } y = 0, \quad u = 0 \text{ for } y = 1.$$

The flow model (33) is closed and completed by respective boundary conditions dependent on the stage. The flow $-q$ in the saturated zone ($u = 1$) is given by the R.H.S. in (16) (in Stage 4 by the R.H.S. in (28)).

It is quite natural to apply the MOL method (space discretization) in (33), (17), (18), and (16) and to reduce it to a system of ODEs or DAEs (since the algebraic equation (18) may be included, too). For a good approximation in a neighborhood of the wetting front we consider grid points

$$0 = y_0 < y_1 < \cdots < y_i < \cdots y_N = 1, \quad \alpha_i = y_i - y_{i-1} \tag{35}$$

so that $\alpha_i = \gamma \alpha_{i-1}$ with $\gamma \leq 1$. Let us define $y_{i-\frac{1}{2}} := \frac{y_i + y_{i-1}}{2} = y_{i-1} + \frac{\alpha_i}{2}$ for $i = 1, \ldots, N$ and integrate the equation (33) over the interval $I_i = (y_{i-\frac{1}{2}}, y_{i+\frac{1}{2}})$ for $i = 1, \ldots, N-1$; here we use the notation $u_i(t) \approx u(y_i, t)$. The rectangle rule gives

$$\int_{I_i} \theta_0 \partial_t u(x,t)) dx \approx \frac{\alpha_i + \alpha_{i+1}}{2} \theta_0 \partial_t u_i(t). \tag{36}$$

We approximate the derivatives using central differences

$$\begin{aligned} \partial_y u(y,t)|_{y=y_{i+\frac{1}{2}}} &\approx \frac{u_{i+1}(t) - u_i(t)}{\alpha_{i+1}} := \partial_y u_i^+, \quad \partial_y u(y,t)|_{y=y_{i-\frac{1}{2}}} \\ &\approx \frac{u_i(t) - u_{i-1}(t)}{\alpha_i} := \partial_y u_i^-, \end{aligned} \tag{37}$$

and use the notation $WD_{i-\frac{1}{2}} = WD(u(y_{i-\frac{1}{2}}))$ and $k_{i-\frac{1}{2}} = k(u(y_{i-\frac{1}{2}}))$ for $i = 1, \ldots, N$. The derivative $\partial_y u$ is approximated by the derivative of the Lagrange polynomial $(L_i(y))$ passing through the points (y_{i-1}, u_{i-1}), (y_i, u_i), and (y_{i+1}, u_{i+1}) (to approximate $\partial_y u_0$ or $\partial_y u_N$ included in the boundary conditions we take the Lagrange polynomial passing through the points (y_0, u_0), (y_1, u_1), (y_2, u_2) or (y_{N-2}, u_{N-2}), (y_{N-1}, u_{N-1}), (y_N, u_N)). Then, our approximation of (33) reads as follows

$$\begin{aligned} \partial_t u_i = &\frac{2K_s}{\theta_0(\alpha_i + \alpha_{i+1}) ss^2} [WD_{i+\frac{1}{2}} \partial_y u_i^+ - WD_{i-\frac{1}{2}} \partial_y u_i^- + ss(k_{i-\frac{1}{2}} - k_{i+\frac{1}{2}})] \\ &+ \frac{\partial_t s_1 (1 - y_i) + \partial_t s_2 y_i}{ss} \partial_y L_i(y_i), \end{aligned} \tag{38}$$

for $i = 1, \ldots, N-1$. We approximate the term $\partial_x u(1,t)^p$ in (17) by $\partial_y L_{N-1}^p(y)|_{y=1}$ where $L_{N-1}^p(y)$ is the Lagrange polynomial passing through the points (y_{N-2}, u_{N-2}^p), (y_{N-1}, u_{N-1}^p), and $(y_N, 0)$.

Finally, if we use the notation

$$Y = [u_1, \ldots u_{N-1}, s_1, s_2, \ell, \ell_2] \tag{39}$$

then our resulting system can be written in the form

$$M(Y,t)\dot{Y} = f(t,Y) \tag{40}$$

and can be solved by a solver for stiff DAEs (e.g., ode15s in the Matlab library).

3.2 Approximation Improvement

To increase the accuracy of our numerical approximations we consider the nonlinear and degenerate Richards equation in terms of both the head and effective saturation. We choose the grid point y_{i_0} and consider the governing equation in pressure head for $i = 1, 2, \ldots, i_0$ and in saturation for $i = i_0 + 1, i_0 + 2, \ldots, N - 1$. Our ODE linked with the grid point y_i has been obtained by applying the finite volume method which is mass conservative. In the approximation of the flux $q_{i-\frac{1}{2}}$ we have to take $D_{i-\frac{1}{2}}, K_{i-\frac{1}{2}}$ requiring $u_{i-\frac{1}{2}}$ which is unknown, and hence we set $u_{i-\frac{1}{2}} = \frac{1}{2}(u_{i-1} + u_i)$. Here, some "up wind" type phenomenon arises. The finite difference type strategy can be more accurate in this case and numerical experiments support it. The governing equation can be written in the form

$$\begin{aligned} \partial_t u &= \frac{K_s}{\theta_0 ss(t)} \left(\frac{(k'(u)h'(u) + k(u)h''(u))(\partial_y u)^2 + k(u)h'(u)\partial_{yy}u}{ss(t)} - k'(u)\partial_y u \right) \\ &\quad + \frac{(\partial_t s_1(1-y) + \partial_t s_2 y)\partial_y u}{ss(t)}, \end{aligned} \tag{41}$$

and in terms of pressure head h in the form

$$\begin{aligned} u'(h)\partial_t h &= \frac{K_s}{\theta_0 ss(t)} \left(\frac{k'(u(h))u'(h)(\partial_y h)^2 + k(u(h))\partial_{yy}h}{ss(t)} - k'(u(h))u'(h)\partial_y h \right) \\ &\quad + \frac{(\partial_t s_1(1-y) + \partial_t s_2 y)u'(h)\partial_y h}{ss(t)}. \end{aligned} \tag{42}$$

We approximate the derivatives $\partial_y h$ and $\partial_{yy} h$ by the derivative of the Lagrange polynomial $(L_i(y))$ passing through the points (y_{i-1}, h_{i-1}), (y_i, h_i), and (y_{i+1}, h_{i+1}) (if we need $\partial_y h_0$ to fulfill boundary conditions we take the Lagrange polynomial passing through the points (y_0, h_0), (y_1, h_1), (y_2, h_2)). The derivatives $\partial_y u$ and $\partial_{yy} u$ are computed using the formula:

$$\partial_y u = \frac{\partial_y (u^p)}{p u^{p-1}}, \tag{43}$$

$$\partial_{yy} u = \frac{\partial_{yy}(u^p) - p(p-1)u^{p-2}(\partial_y u)^2}{p u^{p-1}}, \tag{44}$$

where the derivatives $\partial_y (u^p)$ and $\partial_{yy}(u^p)$ are approximated by the derivatives of the Lagrange polynomial $(L_i^p(y))$ passing through the points (y_{i-1}, u_{i-1}^p), (y_i, u_i^p), (y_{i+1}, u_{i+1}^p), and $p = \frac{1}{2} + \frac{1}{m}$ is the order of degeneracy of the function u at the $s_2(t)$ ($\partial_y u = -\infty$, while $0 > \partial_y (u^p) > -\infty$ at $y = 1$). Thus, in the neighborhood of y = 1 it is suitable to use (43), (44).

3.3 Approximation of Transport-Diffusion and Adsorption

The transport-diffusion and adsorption are realized in the whole sample $(0, s_2(t))$ where water is present. Since the flow characteristics are substantially used in the transport and adsorption model, we use the same grid points in the space discretization as in the flow in

$(s_1(t), s_2(t))$. Additionally, we have to add grid points in the fully saturated part $(0, s_1(t))$. Then we apply the MOL method. Again (for simplicity) we denote by $\{y_i\}_{i=0}^M$ the grid points where $\{y_i\}_{i=0}^M$ belong to $[0, s_1(t)]$. The flux q_w of mass of the contaminant dissolved in the water is expressed by (see (10))

$$q_w = qw - \frac{\theta}{sp} D\partial_y w, \tag{45}$$

where $sp = s_1(t)$ in the fully saturated zone and $sp = s_2(t) - s_1(t)$ in the partially saturated zone. Further, we assume that the first M grid points are moving and follow s_1. The numerical approximation of (10) reads as

$$\theta_i \partial_t w_i + \frac{(q_i sp - D_0 \partial_y \theta_i - \alpha_L \partial_y q_i)\partial_y L_i(y_i) - (D_0\theta_i + \alpha_L q_i)\partial_{yy} L_i(y_i)}{sp^2} - \frac{TC}{sp}(\partial_y \theta_i w_i + \partial_y L_i(y_i)\theta_i) = -\rho \partial_t S_i, \tag{46}$$

where L_i is the Lagrange polynomial passing through the points (y_{i-1}, w_{i-1}), (y_i, w_i), (y_{i+1}, w_{i+1}), and

$$TC = \begin{cases} \partial_t s_1(1 - y_i) + \partial_t s_2 y_i & : \# \text{ in the partially saturated zone;} \\ \partial_t s_1 y_i & : \# \text{ in the fully saturated zone.} \end{cases} \tag{47}$$

Similarly, we approximate the adsorption part of our system

$$\partial_t S_i = \kappa(\Psi(w_i) - S_i) + \frac{TC}{sp} \partial_y \bar{L_{Si}}(y_i), \tag{48}$$

where $\bar{L_{Si}}(y)$ is the Lagrange polynomial passing through the points (y_j, S_j), $j = i-1, i, i+1$. Flow characteristics appearing in the equations are approximated from the flow model solution by cubic splines. After completing the system by boundary conditions it is solved by a solver for stiff ODEs.

4 Numerical Experiments

In our numerical experiments we solve a realistic model in 1D with the following "standard" parameters

$$K_s = 2.4.10^{-4},\ n = 2.81,\ \alpha = -0.0189, \theta_s = 0.4, \theta_r = 0.02,$$
$$\alpha_L = 1, \kappa = 5,\ a = 1, b = 0.5. \tag{49}$$

In the flow part we consider the van Genuchten–Mualem empirical model and the adsorption is represented by the Freundlich adsorption isotherm.

4.1 Comparison of Our Results with Those by HYDRUS

Here we present some comparisons with the well-known and tested software HYDRUS (see Šimunek et al.) using standard parameters which will be completed by various initial and boundary conditions. We have used the version 4.0 which is available for 1D on the Internet. At first, we consider a clean water column of 10 cm over a 10 cm long sample. The water infiltrates by gravitation into the dry sample for 1400 s. We compare the saturation profile at $t = 1400$—see Fig. 2a. In Fig. 2b we zoomed in the saturation profile in the neighborhood

of the wetness front s_2. The blue and green curves correspond to our method with 401 and 13 grid points, respectively. The red curve is obtained by HYDRUS with 1001 grid points. The green curve between two grid points is a segment since there are no other grid points between them. If we draw the saturation u between the last two computed grid points and take into account the order p of degeneracy in the form

$$u^p(x) := \frac{(x - x_{i-1})u^p(x_i) + (x_i - x)u^p(x_{i-1})}{x_i - x_{i-1}}, \tag{50}$$

then we obtain the brown curve between the last two grid points.
However, the wetting front represented by s_2 is obtained very accurately, because the determination of s_2 is explicitly implemented in our method. This fact supports the strength of the application of interfaces. We note that almost the same results are obtained by HYDRUS with 401 grid points. Less than 101 grid points in HYDRUS lead to higher discrepancies. Using numerical data from HYDRUS (with 1001 grid points) we have reconstructed the time evolution of the interfaces s_2 and s_1; comparisons with our results are drawn in Fig. 2c and d.

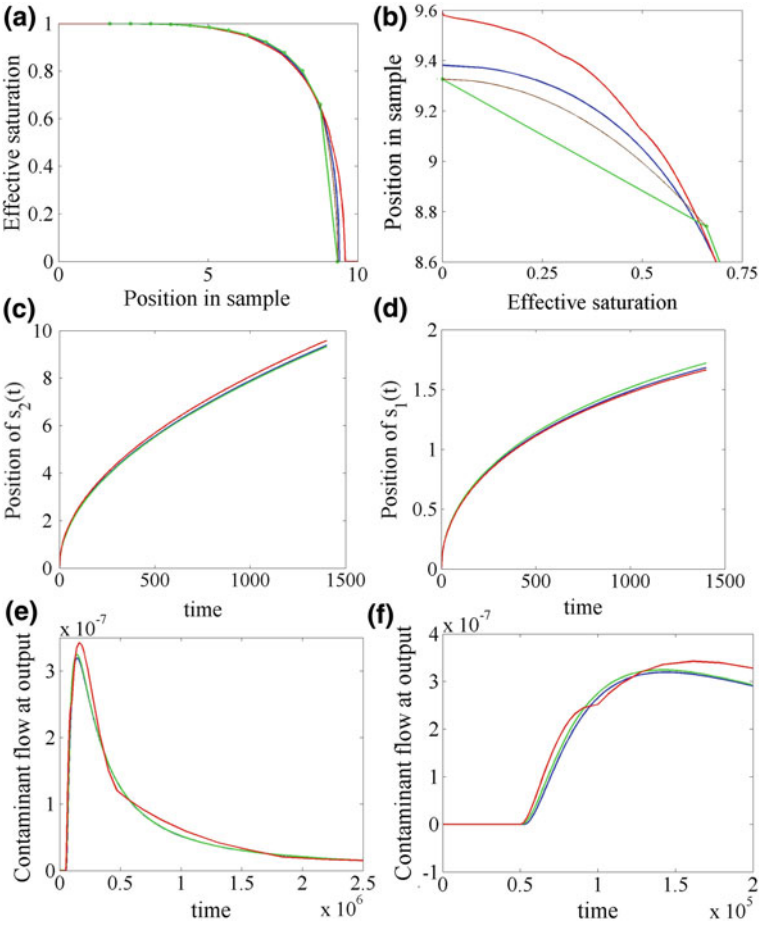

Fig. 2 **a** Profile of saturation at $T = 1400$, **b** zoomed in profile of saturation at $T = 1400$, **c** wetting front s_2; **d** full saturation front s_1, **e** flux of contaminant, **f** zoomed in contaminant flux

The blue and green curves correspond to 401 and 13 grid points in our method, respectively. The red curves correspond to those from HYDRUS. The agreement in s_1 is surprisingly good. In the green curve, the density of grid points is a bit too small near to the s_1 interface. The speed of the s_2 interface produced by HYDRUS is a bit higher than that of our method. In the case of 401 grid points in HYDRUS this difference is about 15 % higher than for the case of 1001 grid points. In Fig. 2e and f we compare the flux of the contaminant in the outflow for time intervals $(0, 2.5.10^6)$ and $(0, 2.10^5)$, where the first part of the curve was zoomed in. These last two figures ((e) and (f)) correspond to contaminant transport of a $3cm$ column of contaminated water. There, some differences are visible, especially in the smoothness of the curves. Similar to previous graphs, the colors correspond to the used software. Unlike in previous graphs, our green curve was obtained using 101 grid points. The (small) lack of smoothness of the red curve is also visible in Fig. 2a. This is strongly visible when comparing gradients and it is reflected in the outflow curves. The mass balance of the water and contaminant are kept in both methods very well. Our method is intended to be used for the solution of inverse problems for adsorption. It will be extended also for centrifugation, too (to speed up the outflow measurements). As our numerical experiments with the water flow into the dry region under centrifugation show, the saturation at the front s_2 is significantly sharper (see also Constales and Kacur 2004) than for the case when only the gravitational driving force is applied. In this case, our method is accurate and efficient.

Some additional comparisons with HYDRUS will be presented in the next section.

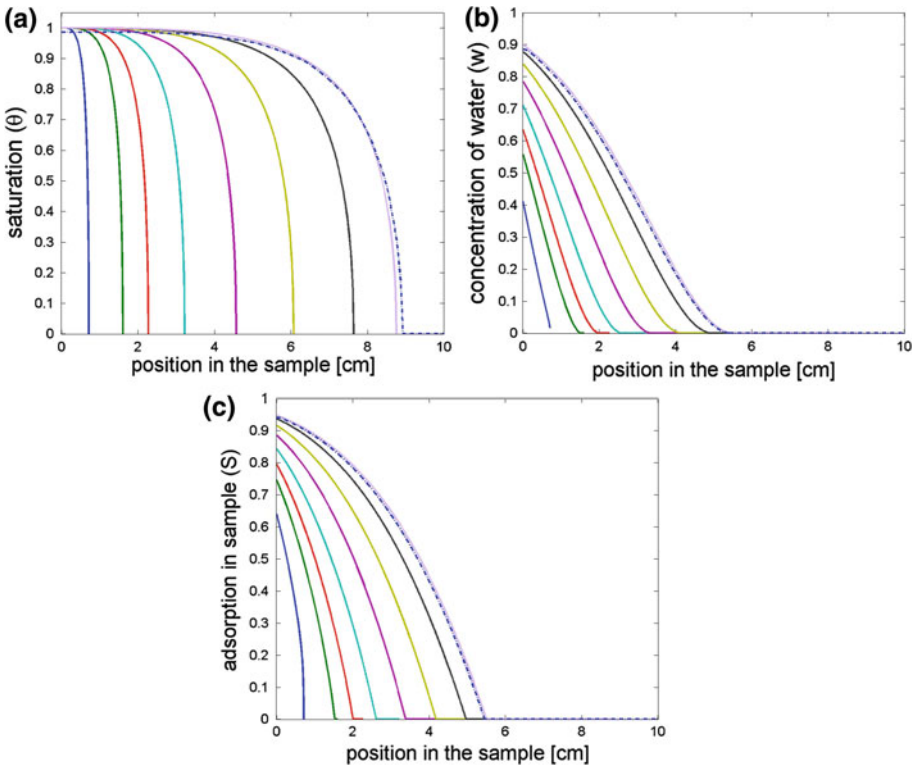

Fig. 3 Time moments used in the following graphs: 10; 50; 100; 200; 400; 700; 1100; and 1436 s. **a** Time evolution of the saturation, **b** Time evolution of the concentration, **c** Time evolution of the adsorption

4.2 Presentation of Our Results in Some Experiments

Consider the contaminated water ($w = 1$) which infiltrates (with gravitational and capillary pressure forces) from a 3 cm column into a 10 cm sample (porous underground).

If some of the "standard" parameters are changed in the following experiments, then we shall note it. **The solutions corresponding to HYDRUS are represented by chain-dotted curves in the following graphs.**

Experiment 1 In this experiment we let the contaminated water infiltrate up to the time when the column is empty. In Figs. 3 and 4 we present the time evolution of the flow (in terms of the effectve saturation), the concentration in the infiltrated water, the amount of the adsorbed contaminant (in the soil), the contaminant mass distribution (in soil, water, and column), and the time evolution of the adsorbed mass of the contaminant in 1 cm clays of the sample. Additionally, we present the time evolution of the interfaces s_1, s_2. This experi-

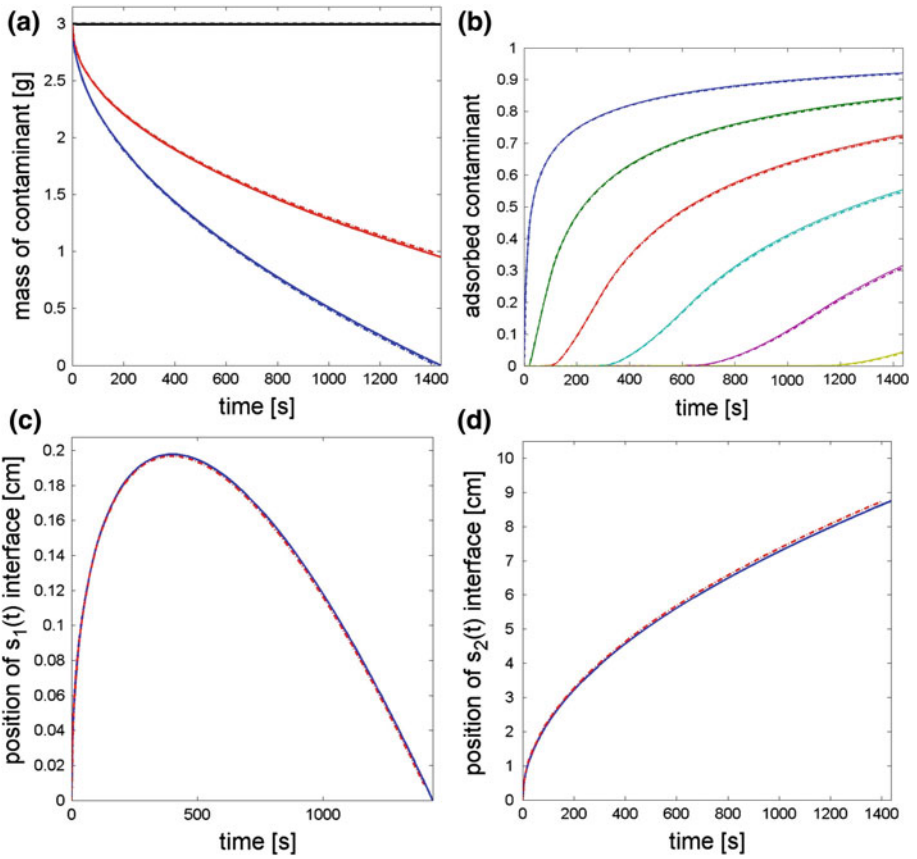

Fig. 4 **a** Time evolution of the contaminant mass distribution: mass in column; mass in column and sample (dissolved in water); total mass in column, sample, and adsorbed contaminant in porous media. **b** Time evolution of the contaminant mass adsorbed in clays in $< i, i+1 >$ $(i = 0, 1, \ldots, 5)$ successively from the top of the sample. **c** Time evolution of the position of the interface $s_1(t)$, **d** Time evolution of the position of the interface $s_2(t)$

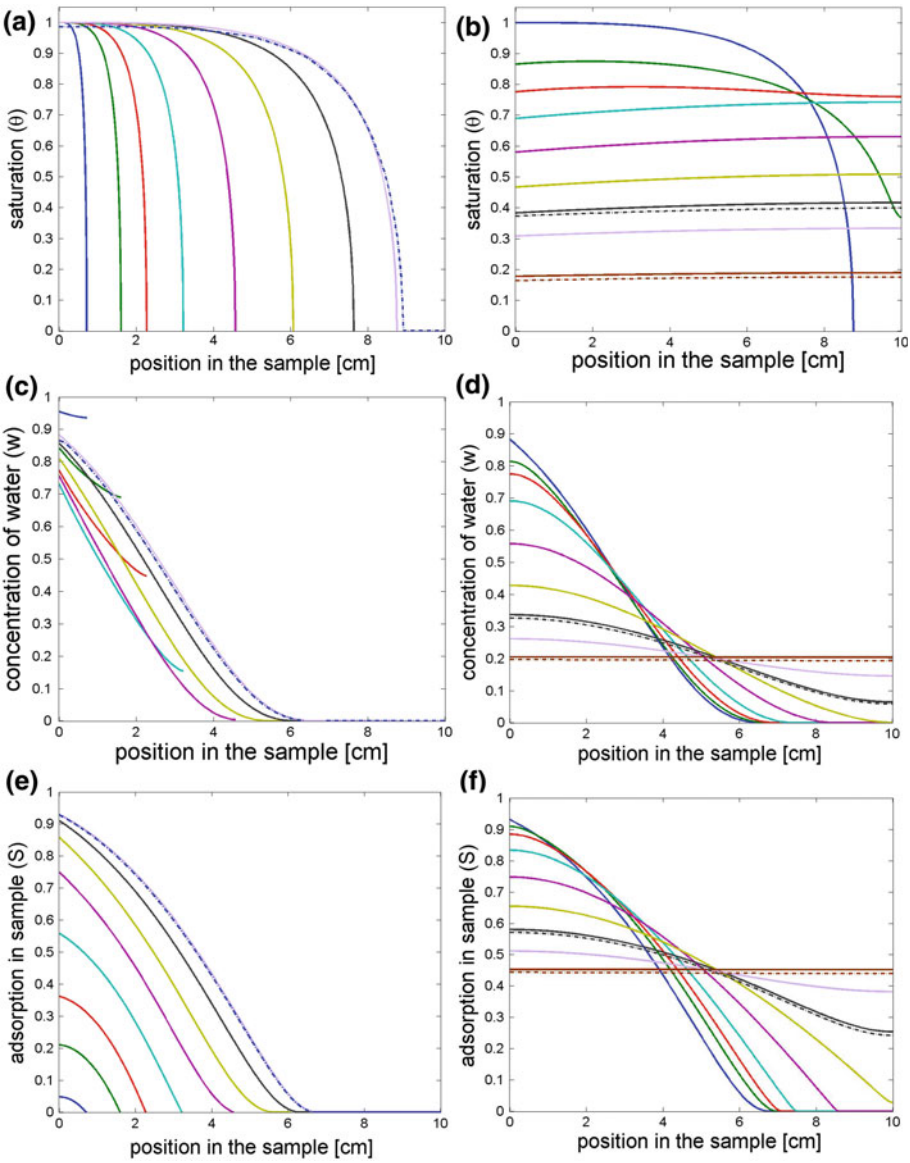

Fig. 5 Time moments used in the graphs (**a**), (**c**), (**e**): 10; 50; 100; 200; 400; 700; 1100; and 1436 s. Time moments used in the graphs (**b**), (**d**), (**f**): 1436; 2000; 3000; 7000; 20000; 50000; 10^5; 2.10^5; and 10^6 s. **a**, **b** Time evolution of the saturation, **c**, **d** Time evolution of the concentration, **e**, **f** Time evolution of the adsorption

ment lasts up to the time when the column is empty. This is realized approximately at time 1436 seconds.

To understand Fig. 4a, make a perpendicular line to the x axis at some time point t. The length of the segment between the x axis and the intersection with the blue curve is the amount of the contaminant present in the column. The length of the segment between the blue curve and the red curve is the amount of the contaminant present in the water that is saturated in

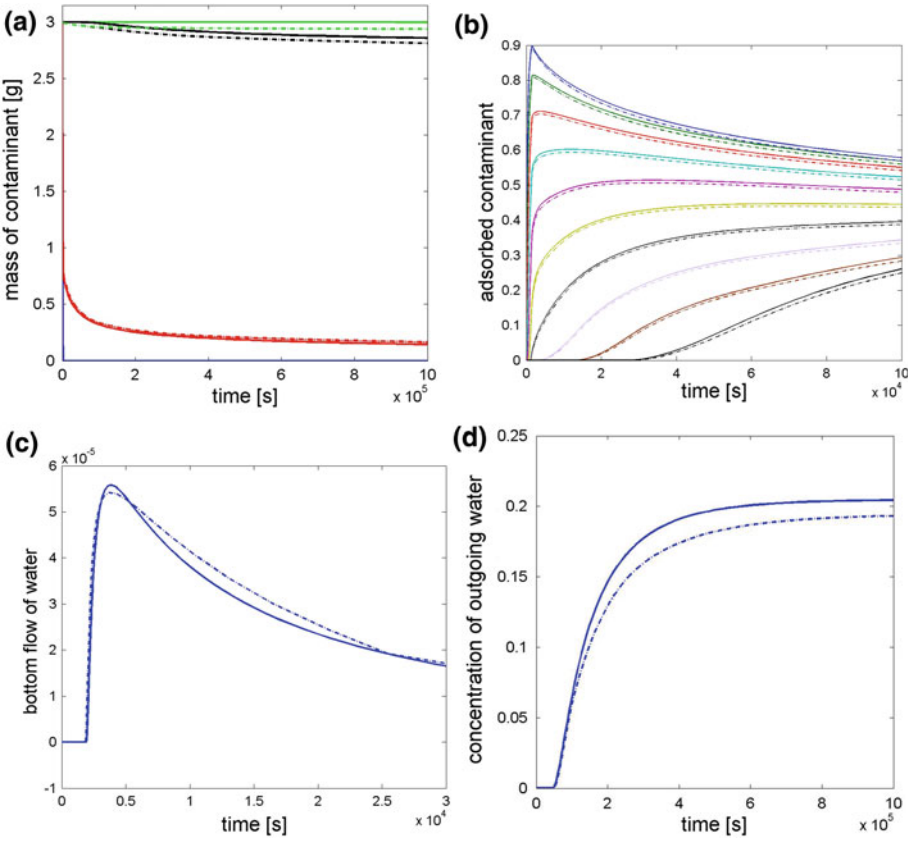

Fig. 6 **a** Time evolution of the contaminant mass distribution: mass in column; mass in column and sample (dissolved in water); mass in column, sample, and adsorbed contaminant in porous media.; total mass in column, sample, adsorbed in porous media and in bottom tube. **b** Time evolution of the contaminant mass adsorbed in clays in $< i, i+1 >$ $(i = 0, 1, \ldots, 9)$ successively from the bottom of the sample. **c** Time evolution of the total outgoing water. **d** Time evolution of the concentration of outgoing water

the sample. Finally, the length of the segment between the red curve and the black top curve is the amount of the adsorbed contaminant by the porous media.

Experiment 2 In our second experiment we let the contaminated water infiltrate from a 3 cm column, but we change the value of κ to $\kappa = 5.10^{-3}$. In this case, we additionally present in figures the time evolution of the outgoing water and its concentration and we omit the time evolution of the interfaces s_1 and s_2. In the experiment, approximately at time 1436 s the column is empty. We present the results of this experiment in Figs. 5 and 6.

It can be seen in Fig. 6c that because of the small value of κ ($\kappa = 5.10^{-3}$), the concentration at the interface $s_2(t)$ is positive for a relatively long time, unlike in previous experiments. However, differences between this experiment and the same experiment with larger values of κ seem to diminish in time, so it may be very difficult to compute the approximate value of κ from data at a later time (i.e., data from the outflow) unless κ is small enough.

5 Conclusions

An accurate and efficient numerical method is developed for the contaminant transport in porous media in 1D applying the MOL method (reduction to ODE (DAE) systems). The accuracy is based on moving grid points in the partially saturated zone which is bounded by moving interfaces representing the full saturation and wetness fronts. Therefore, our method requires only a few grid points to keep the solution accurate. The mathematical model for the time evolution of the wetness front and approximations of gradients of saturation (gradient is infinity at the wetness front) significantly use the order of degeneration linked with soil parameters in the applied van Genuchten–Mualem empirical flow model. This method is a very good candidate for solving the inverse problem where one wants to determine parameters in the adsorption isotherm. Specifically, our method can be used to determine soil parameters. In that case, we can utilize additional measurements data for s_2 (e.g., by gamma rays), since the saturation profile in its neighborhood is very sharp. Comparisons of our results with those obtained by the well-known and well-tested software HYDRUS (based on another method) are in good agreement and also support our method. We note that the method used in HYDRUS can be applied in more dimensions, too. Our method cannot be extended to more dimensional cases directly, except for very special cases in 2D (radially symmetric problems). It is not known how to model interfaces in non-symmetric cases since the interface evolution is significantly affected by its curvature.

Acknowledgments The authors confirm the financial support of the Slovak Research and Development Agency under the contracts APVV-0184-10, APVV-0743-10 and LPP-0204-09.

References

Bear, J., Cheng, A. H.-D.: Modeling Groundwater flow and Contaminant Transport. Springer, ISBN 978-1-4020-6681-8

Bitterlich, S., Knabner, P.: An efficient method for solving an inverse problem for the Richards equation. J. Comput. Appl. Math. **147**(1), 153–173 (2002)

Bitterlich, S., Durner, W., Iden, S.C., Knabner, P.: Inverse estimation of the unsaturated soil hydraulic properties from column outflow experiments using free-form parameterizations. Vadose Zone J. **3**, 971–981 (2004)

Constales, D., Kacur, J.: Determination of soil parameters via the solution of inverse problems in infiltration. Comput. Geosci. **5**, 25–46 (2004)

Constales, D., Kacur, J., Malengier, B.: A precise numerical scheme for contaminant transport in dual-well flow. Water Resour. Res. **39**(10), 1303 (2003)

Kacur, J., Malengier, B., Remesikova, M., et al.: Contaminant transport with equilibrium and non-equilibrium adsorption. Comput. Methods Appl. Mech. Eng. **194**, 489–497 (2005)

Kacur, J., Malengier, B., Trojakova, E.: Numerical modelling of convection-diffusion-adsorption problems in 1D using dynamical discretization. Chem. Eng. Sci. **65**(7), 2301–2309 (2010)

Knabner, P., van Duijn, C.J.: Solute transport in porous media with equilibrium and nonequilibrium multiple-site adsorption, Traveling waves. Journal für die reine und angewandte Mathematik **415**, 1–49 (1995)

Krutle, S., Knabner, P.: A new numerical reduction scheme for fully coupled multicomponent transport-reaction problems in porous media. Water Resour. Res. **41**(9), W09414 (2005)

Krutle, S., Knabner, P.: A reduction scheme for coupled multicomponent transport-reaction problems in porous media: generalization to problems with heterogeneous equilibrium reactions. Water Resour. Res. 43 (2007)

Šimunek, J., Nimo, J.R.: Estimating soil hydraulic parameters from transient flow experiments in a centrifuge using parameter optimization technique. Water Resour. Res. **41**, W04015 (2005)

Šimunek, J., Šejna, M., van Genuchten, M.T.: The HYDRUS-1D software package for simulating the one-dimensional movement of water, heat, and multiple solutes in variably/saturated media, version 2.0, Rep. IGWMC-TPS-70, 202 pp., Int. Groundwater Model. Cent., Colo. Sch of Mines, Golden, Colo.

Totsche, K.U., Knabner, P., Kgel-Knabner, I.: The modeling of reactive solute transport with sorption to mobile and immobile sorbents part II: model discussion and numerical simulation. Water Resour. Res **32**(6), 1623–1632 (1996)
Sun, N.-Z.: Inverse Problems in Groundwater Modelling. Kluwer, Academics, Dordrecht (1994)
Sun, N.-Z.: Mathematical Model of Groundwater Pollution. Springer, New York (1966)
van Genuchten, M.T.: A closed-form equation for predicting the hydraulic conductivity of unsaturated soils. Soil Sci. Soc. Am. J. **44**, 892–898 (1980)